Energy-efficient unburned technologies for the use of phosphogypsum

S N Zolotukhin[1], O B Kukina[1], A A Abramenko[1], E A Soloveva[1] and E A Savenkova[1]

[1]Voronezh State Technical University, Moscow Avenue, 14, Voronezh, 394026, Russia

E-mail: lgkkn@rambler.ru

Abstract. Along with the traditional ways of using the waste of chemical production of sulfuric acid - phosphogypsum, the innovative and promising way is its processing in the production of cementless, non-flaming, artificial building materials. In this paper, the theoretical foundations of the technology for the preparation of limestone-sand-phosphogypsum building material (IPF), the influence of the thickness of aqueous films on the processes of structure formation, the results of studies on the physicomechanical properties, nano- and microstructure of the IPF are presented. It is shown that, as in polymer materials, where this effect was observed, the strength is created due to the presence of water films with nanoscale thickness. The developed technology of non-burning cementless IPF building materials will allow to reduce and completely abandon the labour, energy, time-consuming processes of roasting, washing of phosphogypsum, which is actual, promising and innovative in the conditions of energy and resource saving. Products made with the use of this technology will reduce the energy consumption for heating the premises.

1. Introduction

There are different ways of processing phosphogypsum. For example, compounds from phosphogypsum, cement, slag, ash and other active additives have found wide application [1-4]. Compositions are studied with the addition of phosphogypsum to the cement clinker [5-8]. One of the innovative trends in the production of building materials is the production of unroasted cementless artificial composites [9-14].

At present, the authors of the article develop the technology of unroasted cementless building materials on the basis of phospho-gypsum, which requires correction for starting the production of wall partitions on the industrial scale. The advantage of the technology being developed over the existing ones is lower labor-, energy-, time-consumption, as well as reducing the cost of the final material due to the use of cheap mixture components [15].

Phospho-gypsum is a large-capacity waste for producing sulfuric acid. Despite the considerable amount of researches on the utilization of phospho-gypsum, only 0.3 million tons or 1.5% from its 20 million tons produced annually, find use, the rest is removed from the territory of enterprises as waste, which is associated with considerable labor consumption and financial expenses [16].

It is known that in phospho-gypsum dihydrate, the content of $CaSO_4 \cdot 2H_2O$ is 80 ... 98%, and in gypsum rock pre-dried to constant volume, the content of $CaSO_4 \cdot 2H_2O$ should be no less than 95, 90, 80 and 70%, respectively, for the 1st, 2nd, 3rd and 4th kinds, according to GOST 4013 -82.

Due to the high content of dihydrate gypsum in phospho-gypsum dihydrate, numerous studies on its reprocessing were aimed at getting gypsum on classical techniques: roasting, boiling in gypsum

digesters, and autoclaving. These studies have not led to a widespread use of phospho-gypsum. Waste of phospho-gypsum continues to be stored in dumps, which requires large amounts of soil and is of an ecological problem. The previous studies have proved that instead of the expensive washing of phospho-gypsum dihydrate, it is rational to use lime additives, which are strongly bind acid residues [17, 18].

The technology of producing unroasted cementless building materials on the basis of phospho-gypsum is based on the imagination of the mechanism of the water film thickness influence on the processes of structural formation between the nano- and micro-sized particles of the construction composite.

Water is the dispersion medium in which the interactions of particles take place, and the medium predetermines the interaction forces between the composite particles.

The influence of water films on the stability of colloidal systems that are present in the lime-and-sand-phospho-gypsum material (LSPh) may be defined from the viewpoint of chemical thermodynamics as follows.

Figure 1 shows that in hydrophilic systems with slow convergence of the particles of the dispersed phase, the liquid layer between them will first be decreased without the work expense and changing the free energy of the ΔF system. However, beginning from a distance $\Delta = 2\delta$ (δ - the value of water-polymeric shell around each of the particles), it is necessary to take into account the forces of intermolecular interaction of the dispersion medium and dispersed phase [14].

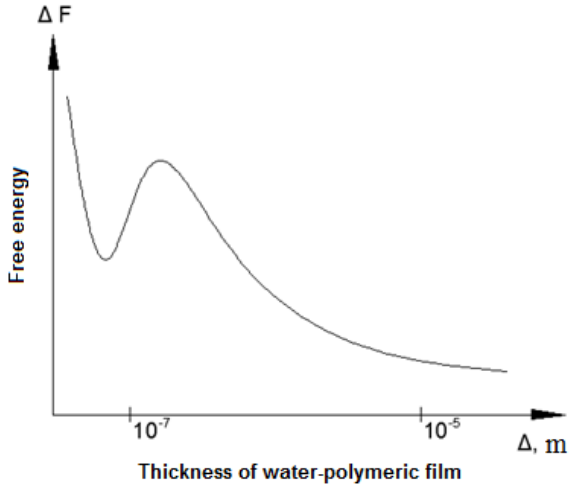

Figure 1. Change of free energy depending on the water-polymeric film thickness for hydrophilic particles (according to [14])

The quantity of Δ layer depends on the degree of this interaction. This occurs in the case of significant forces of molecular adhesion promoting the convergence of the particles of the dispersion medium and the dispersed phase with $\Delta \geq 1 \cdot 10^{-7}$m. Further slow convergence of particles causes an increase of the excess of ΔFu, free surface energy, consequently, it can not proceed spontaneously. Therefore, particle convergence requires the application of energy, which, in our experiments, has been created by the application of the external pressure.

The stability of such a colloidal system is caused by the wedging pressure arising in the liquid interlayer between the particles of the dispersed phase.

Figure 2 shows that the excess of the free energy is systematically increased as the particles converge under the influence of external forces, reaching a maximum at a value of $\Delta \approx 10^{-8} \ldots 10^{-9}$ m.

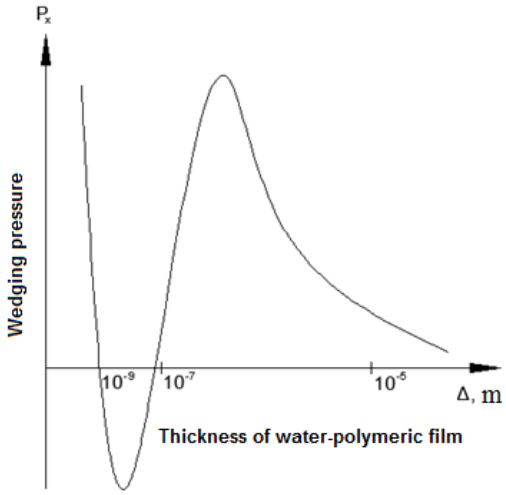

Figure 2. Change of the wedging pressure, depending on the thickness of the water-polymeric film for hydrophilic particles (according to [14]).

Beginning from this distance, ΔF drops rapidly, and the wedging pressure, passing through zero, becomes negative. This case corresponds to the predominance of the cohesion forces, the interlayer spontaneously by jump thins, and in the end the particles of dispersed phase are adhered.

The thickness of the liquid layer, in which an excess of the free energy is not changed, is 10^{-7} m. with a very weak molecular interactions of the dispersed phase with the dispersion medium (the second case). Accordingly, the wedging pressure of the $\Delta \approx 10^{-7}$ m value is zero. With further slow convergence of the particles, the excess of the free surface energy is reduced (the wedging pressure is negative), which corresponds to the loss of stability and spontaneously occurring processes of particles adhesion [14, 19, 20].

While mixing the components of the raw mixtures, water is adsorbed in the films on hydrophilic particles. The mixing of the compositions with a hydrophilic filler is only possible when films are of value in the range of 10^{-7} m $< \Delta < 10^{-5}$ m. For the hydrophilic fillers, in the range of 10^{-7} m $> \Delta > 10^{-9}$ m, there will be achieved the maximum values of strength, density and chemical resistance [14].

When the temperature changes, water-polymeric films sharply change the thickness. At a temperature of 65 ... 70 °C the thickness of water-polymeric films sharply drops to a monolayer, which affects the decrease in the stability of hydrophilic colloid systems. At the same temperatures, penetrating power of water sharply increases, resulting in the destruction of rocks [19].

The reversibility of the temperature dependence on the stability of the water dispersions points to the reversibility of the structural rearrangement of the boundary layers. These properties of water films should influence the modes of heating the cementless unclinkered building composites, and the properties of the materials obtained in the operation with different temperature regimes as well.

There is a certain value of the film size, which will be optimal for getting the most durable and resistant compositions, and having minimal shrinkage. But in practice, the actual technology does not allow precise control of film thickness. The pH of the aqueous extract also influences the change in the thickness of the water film. Figure 3 shows the dependence of changing the water film thickness on the surface of the quartz grain of the pH value in the range from 2 to 8. The reason for this influence is the change of the long-range of the structural repulsive forces that stabilize the dispersion. The stabilization of the dispersions at low 3 ... 6 pH is associated with increasing the number of surface OH^- groups, capable of forming hydrogen bonds with water molecules, which leads to an increase of the repulsive forces. In conventional washing methods, acid residues and water-soluble compounds of fluoride and phosphoric acid enter into a crystalline structure, are firmly held therein and allow water to be removed from the structure of phospho-gypsum dihydrate, which results in higher energy expenses when boiled by conventional techniques. The introduction of lime changes the acidic structure within the crystal

lattice of the stone, and the rearrangement of nano- and microstructures takes place. Raising the temperature causes weakening the net of directed hydrogen bonds in the water, that reduces the long-range action of the structural forces and leads to the increase of dispersions stability. This property of water films can have great influence on blending the raw mixtures for obtaining composites [14] (according to [14])

.

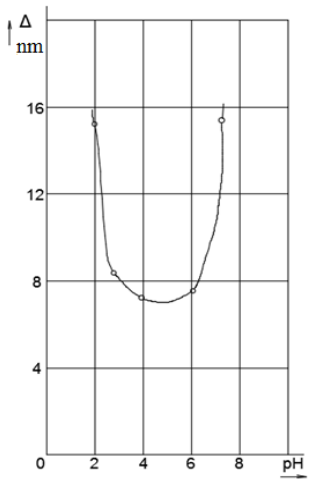

Figure 3. Dependence of the boundary layer thickness on quartz grains on pH

In connection with the above-said, the aim of this work is to analyze the data obtained on the influence of water films thickness on the processes of structural formation between the nano- and micro-sized particles in the LSPh composite building material. The methods of X-ray-phase analysis and scanning electron microscopy have been used.

2. Materials and methods

The following components were used for preparing the raw mixture:
-building quicklime (manufacturer: Rossosh, "Pridonhimstroyizvest"; packing: Voronezh, "Stroitorgservice";
- stale dihydrate waste phospho-gypsum of Uvarovskii chemical plant, liquidated in 2000 because of bankruptcy. Area dumps is 6.4 km^2, the volume reaches about 35 million tons.;
- sandy loam with the specific surface of 4000 - 4500 cm^2/ g from the quarry of Tambov region, Uvarovskii district located in the immediate vicinity from the phospho-gypsum deposits.

The data of the granulometric analysis of foundry sand components are presented in Table 1.

Table 1. Results of granulometric analysis of molding sand components

Name of residue	Residues % by weight					Passage through a sieve with mesh 0.16% by weight
	2.5	1	0.63	0.315	0.16	
			Phospho-gypsum			
Private	13.78	8.74	9	17.86	30.82	19.8
Full	13.78	22.52	31.52	49.38	80.2	-
			Sandy loam			
Private	6.58	9.2	16.36	43.22	20.34	4.3
Full	6.58	15.78	32.14	75.36	95.7	-
			Quicklime			
Private	74.68	7.24	2.22	4.44	5.86	5.56
Full	74.68	81.92	84.14	88.58	94.44	-

Water-concretion ratio (W/C) of the composition being studied was chosen from the condition easy for molding and obtaining defect-free samples. Hydro-mechanical-and-chemical activation was carried out in the laboratory MLA-30 mixer with the frequency of the blade rotation about its axis 126 rpm, the maximum heating temperature is (200 ± 5) °C.

The pH value was determined using ionomer I-160. Physical-and-mechanical properties of the samples were determined in accordance with the requirements of All-Union State Standard (AUSS) 23789-79, AUSS 8736-93, AUSS 5802-86, AUSS 310.4.81, AUSS 22 AUSS 688-77, 125-79.

The weighting characteristics were determined by means of the electronic laboratory balances PH-3413 to the nearest 1 g.

Molding of the cylinder-specimens of 5 × 5 cm dimensions was made using a hydraulic press PSU-125. The ultimate compressive strength of the cylinder-specimens aged of 1, 3, 7, 14 and 28 days were determined with the use of the universal electromechanical test system Instron 5982, the load error is ± 0.5%. Water absorption and water resistance were determined in accordance with AUSS 6428-83, AUSS 8462-75.

Table 2 shows the chemical composition of the raw mixture components.

Table 2. Chemical composition of the raw mixture solid components

Chemical composition,%	Name of the solid component of the raw mixture		
	Phospho-gypsum	Sandy loam	Lime
Al_2O_3	0.46	14.04	0.32
SiO_2	1.66	69.35	1.08
CaO	33.58	3.52	62.30
Na_2O	0.60	0.73	0.04
MgO	0.12	1.66	1.27
P_2O_5	1.28	0.29	0.02
K_2O	0.16	3.10	0.09
TiO_2	0.06	0.96	-
Fe_2O_3	0.81	5.55	0.26
MnO	-	0.09	0.01
S	31.26	0.16	0.07
C	26.57	-	23.12
H_2O	-	-	11.11

X-ray phase analysis was carried out on PANalytical EMPYREAN automatic diffractometer using Cu Kα1 radiation (hybrid Ge {111} primary beam monochromator) and a position-sensitive detector PIXcel1D. The measurement was performed in the reflection mode, θ/2θ scan pitch at 0.026° on 2θ. The measuring range is 15 – 80° 2θ. The calculation of interplanar spacings and integrated intensities used for improving the cell parameters was carried out according to the profiling analysis of the experimental diffraction patterns (the Pauli method). The phase analysis was conducted using the "powder" database PDF-2 ICDD (International Centre for Diffraction Data). All the calculations to improve the diffraction patterns, identifying and improving the cell parameters, determining the phase composition were carried out with the use of program system HighScore Plus, Version:3.0.t (3.0.5), Date 30-01-2012. Produced by: PANalytical B.V. Amelo, The Netherland.

A scanning electron microscope of JEOL brand designed to produce an image of the object surface with high (up to 0.4 nm) spatial resolution was used for the microscopic analysis.

The mixture for molding was prepared as follows: sandy loam with phospho-gypsum was poured and blended in a mixer with heating temperature at 60 ... 80 °C. At the same time, in another container, lime was quenched with hot water and was added to the dry ingredients in the quenching process. Then, all the ingredients were mixed until obtaining a homogeneous mass at a temperature not less than 60 °C. Then, the obtained mixture was pressed under a pressure of 1 ton for cylinder-specimen. The choice of pressing pressure was conditioned by the pressure of standard equipment for the production of sand-lime brick. Gaining strength of the specimens took place in normal wet conditions of hardening. To

reveal the optimal composition of the raw mixture, a planning matrix was created, there were investigated the interrelations between the percentage of the components and ultimate compressive strength of the specimens, and the water absorption and softening coefficients as well. The results of the investigation are presented in Table 3.

3. Results and discussion

Table 3 shows some of the properties of LSPh unroasted cementless composite building material.

Table 3. Properties of LSPh unroasted cementless composite building material

Composition №	Composition			Ultimate compressive strength (28 days), MPa	W/ S	Density, кg/м^3	Coefficient of water absorption	Coefficient of softening
	Lime, %	PHG, %	Sandy loam, %					
1	50	50	0	2.35	0.78	1507	0.34	0.50
2	40	50	10	2.89	0.40	1513	0.31	0.38
3	30	50	20	4.05	0.46	1716	0.26	0.57
4	20	50	30	3.34	0.36	1728	0.27	0.38
5	10	50	40	4.43	0.30	1766	0.23	0.52
6	0	50	50	3.33	0.17	1788	-	-
7	40	60	0	2.03	0.60	1517	0.34	0.42
8	30	60	10	2.41	0.58	1593	0.28	0.51
9	20	60	20	4.14	0.40	1680	0.25	0.55
10	10	60	30	4.76	0.30	1734	0.23	0.63
11	0	60	40	3.96	0.15	1755	-	-
12	30	70	0	1.97	0.50	1565	0.32	0.57
13	20	70	10	3.23	0.50	1642	0.29	0.52
14	10	70	20	2.32	0.31	1657	0.28	0.56
15	0	70	30	3.50	0.20	1723	-	-

In the 6th, 11th, 15th compositions containing no lime, mold appeared on the sample surface at gaining the strength in normal-wet conditions, therefore, the composition can not be used for manufacturing building articles.

In the 1st, 7th, 12th compositions containing no sandy loam, the samples of the 1st composition (50% lime, 50% phosphor-gypsum) had the maximum compressive strength.

As a result of water saturation of LSPh composite material, the average density and the ultimate compressive strength are decreased.

Thus, the water absorption coefficient is increased in proportion to the content of lime and sandy loam. At a constant content of phospho-gypsum, the minimal water absorption is observed in 10% of lime in the LSPh composition, which corresponds to the 5th, 10th, and 14th ones.

At the constant content of 50%, 60%, 70% of phospho-gypsum and variable lime and sandy loam, the indexes of the strength reach the maximum of 4 ... 5 MPa at 10… 20% of lime and 30 ... 40% of sand.

Gaining the strength of the investigated compositions in normal-wet conditions took place according to the following relationship: the 3rd day - 50% of the final strength, the 7th day - 65% of the final strength, the 14th day - 70% of the final strength, the 21st day - 80% of the total strength, the 28th day – the strength is 100%.

The diagram of gaining strength is shown in figure 4.

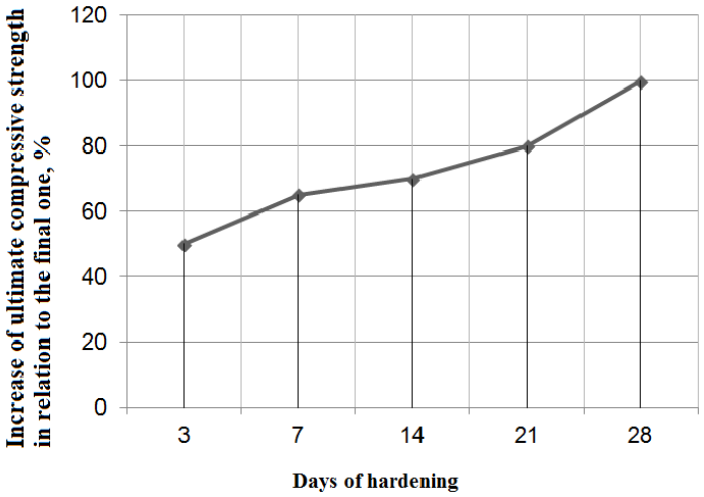

Figure 4. Gaining strength of the investigated compositions in normal-and-wet conditions

It is found that the samples at hardening in normal-and-wet conditions reach only 40% of the final ultimate compression strength under dry conditions.

It is necessary to take into account the fact that lime is the most expensive one of the components used, and from the data obtained, the optimal ratio of strength, the economic effect, the water absorption and softening coefficients are achieved in the 10th composition (10% of lime, 60% of phospho-gypsum, 30% of sandy loam).

To determine the physical-and-chemical properties of the samples with the best physical-and-mechanical properties, there was carried out the X-ray phase analysis (XRA) and microscopic research in a scanning electron microscope. The research results are presented in Figures 5 - 10.

Figure 5. shows the diffraction pattern of a quicklime sample (produced in "Pridonhimstroyizvest", Rossosh), which mainly includes the calcium oxide phase CaO with a cubic crystal lattice a = 4.81 Å with interplanar spacings d = 2.77; 2.40; 1.70; 1.45; 1.38; 1.20 Å.

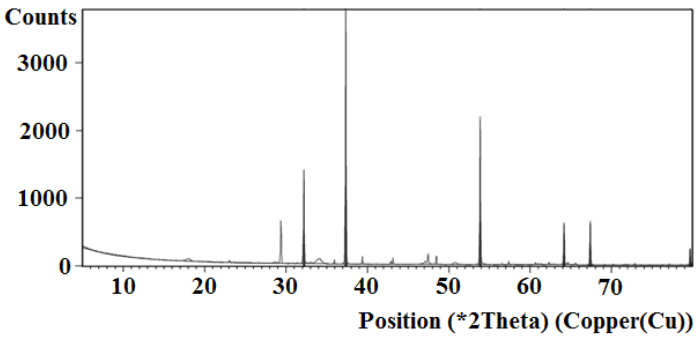

Figure 5. The diffraction pattern of the quicklime sample produced in "Pridonhimstroyizvest", Rossosh

Figure 6 shows the diffraction pattern of the sandy loam sample produced in Uvarovskii district, Tambov region, which includes the following phases:

a) silicon oxide SiO_2 as α-quartz having a hexagonal crystal lattice a = 4.62 Å; b = 4.62 Å; c = 5.21 Å with the interplanar spacings of d = 2.59; 2.86; 3.18; 4.02 Å;

b) hydrosulfate of $FeOHSO_4$ iron with the orthorhombic crystal lattice a = 3.66 Å; b = 6.41 Å; c = 7.15 Å with the interplanar spacings of d = 3.47; 3.65; 4.96 Å;

c) calcium aluminum silicate $Al_3Ca_{0.5}Si_3O_{11}$ monoclinic crystal lattice a = 5.25 Å; b = 8.89 Å; c = 19.48 Å with the interplanar spacings of d = 3.23; 3.76; 4.46 Å.

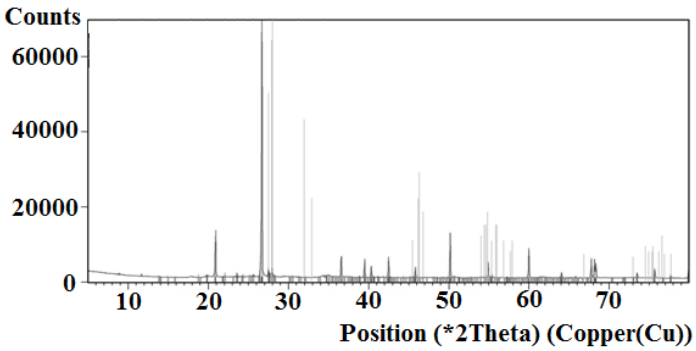

Figure 6. Diffraction pattern of sand produced in Uvarovskii district Tambov region

Figure 7 shows the diffraction pattern of the phosphor-gypsum sample produced at the chemical plant in Uvarovo town, Tambov region, containing the following phases:
a) plaster of Paris $CaSO_4 \cdot 0{,}5\ H_2O$ with a hexagonal crystal lattice a = 6.93 Å; b = 6.93 Å; c = 6.34 Å ,with the interplanar spacings of a = 7.61; 6.28 Å; b = 15.20 Å; c = 6.52 Å;
b) gypsum dihydrate $CaSO_4 \cdot 2\ H_2O$ with monoclinic crystal lattice a = 7.61; 6.28 Å; b = 15.20 Å; c = 6.52 Å with the interplanar spacings of d = 7.63; 3.07; 2.87; 2.68; 2.12 Å.

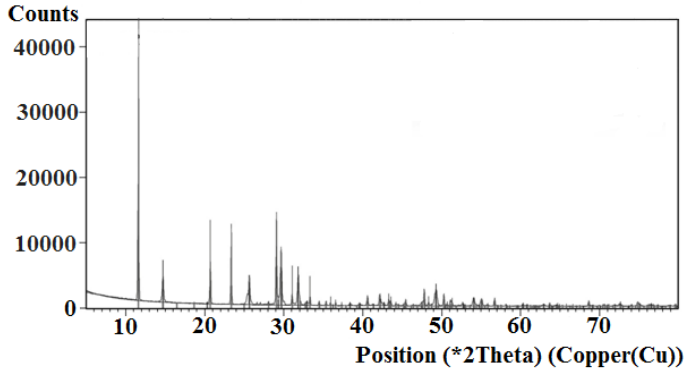

Figure 7. Diffraction pattern of phosphor-gypsum produced in Uvarovskii district, Tambov region

Figure 8 shows the diffraction pattern of a sample of a cementless unroasted sand-lime-phospho-gypsum composite building material, represented by the following phases:
a) quartz with the hexagonal crystal lattice a = 4.62 Å; b = 4.62 Å; c = 5.21 Å with the interplanar spacings of d = 3.34; 2.45; 1.98; 1.67 Å;
b) dihydrate gypsum $CaSO_4 \cdot 2\ H_2O$ with monoclinic crystal lattice a = 7.61; 6.28 Å; b = 15.20 Å; c = 6.52 Å with the interplanar spacings of d = 7.63; 3.07; 2.87; 2.68; 2.12 Å;
c) calcium carbonate $CaCO_3$ with a hexagonal crystal lattice a = 4.98 Å; b = 4.98 Å; c = 17.07 Å with the interplanar spacings of d = 3.03; 2.49; 2.28; 2.09; 1.91; 1.87 Å.

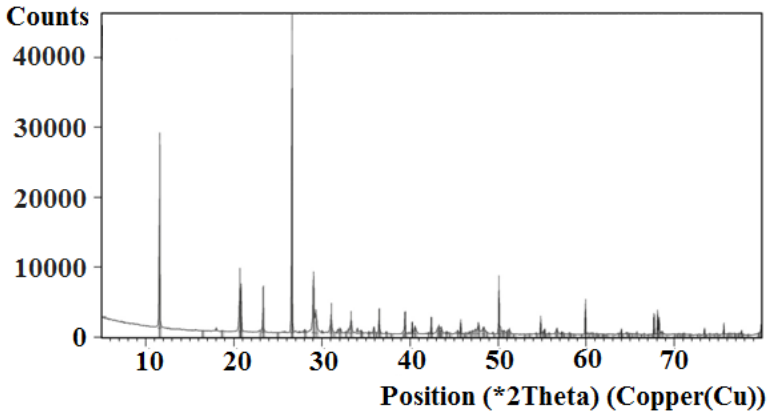

Figure 8. Diffraction pattern of the LSPh cementless unroasted composite building material

When comparing the diffraction patterns of initial raw materials and the LSPh cementless unroasted composite building material, one can conclude that in the composite there has disappeared the phase of plaster of Paris which was observed in phosphor-gypsum because of the hydration processes of plaster of Paris with converting it into the dihydrate one. The part of the portlandite phase is converted into the phase of calcium carbonate during the chemical processes at the expense of carbonation.

The X-ray-phase analysis of phospho-gypsum dihydrate and the LSPh composite material did not reveal the presence of the products of the lime neutralization of acid residues – water-soluble phosphorus and fluorine compounds, which being a part of the crystal lattice, may affect the composite structural formation processes.

Figures 9 and 10 show the microstructure of cementless unroasted lime-sand phosphor-gypsum composite material from which one can notice that the system of composition is represented by the crystals of portlandite, quartz crystals joined in the form of druses by the crystallization planes and phospho-gypsum crystals forming a framing reinforcing structure. Figure 11 shows multiple contacts of joining, concretion, penetration between individual crystals of different phases: of portlandite (in the form of prisms), of quartz (in the form of layered planes) and of phosphor-gypsum (in the form of needles).

The particles of lime, clay, fluorides, phosphates, sulfates, hydrogen sulfates, due to their high dispersion, fill the space between the phospho-gypsum dihydrate crystals, providing optimal thickness of water films that can be well seen in figures 9 and 11.

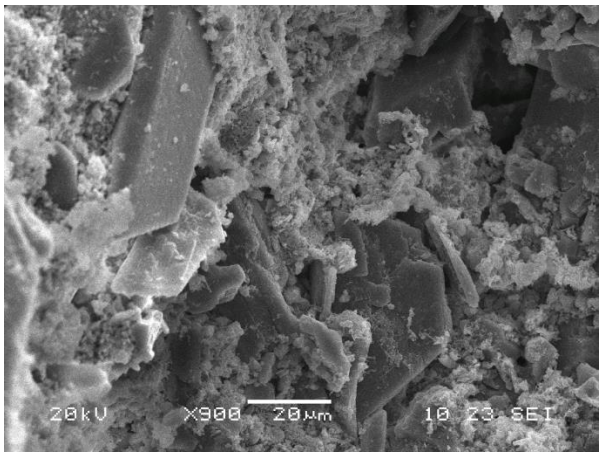

Figure 9. Microstructure of the LSPh cementless unroasted composite building material

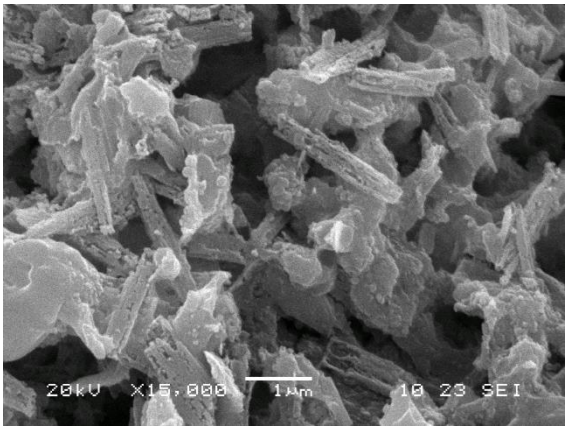

Figure 10. Framing reinforcing crystal phospho-gypsum structure

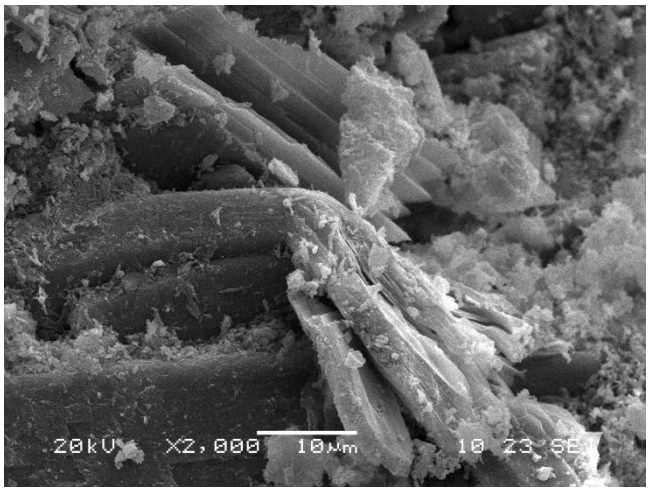

Figure 11. Contacts of joining, concretion, penetration between individual crystals of different phases

According to the rule of isomorphism, unit cells of portlandite and quartz crystals have the parameters that do not differ in size by more than 15%, therefore, joint crystallization surfaces are formed between them in high pressure conditions, as for needle-shaped crystals of phosphor-gypsum, they develop additional contact zones at the expense of framing net. Besides, water films with a thickness of approximately 1·10-7 m are involved in the structural formation of LSPh composite, there appear van der Waals forces of the interactions and some voids in the material are filled with nano-micro-dispersed particles of lime, clay and other particles. That was confirmed by X-ray-phase analysis.

Figure 11 shows that the distance between some of the crystallization surfaces reach approximately 1 · 10-7 m. The micrographs obtained well confirm the hypothesis of the applicability of the dependencies considered in Figures 1 - 3 for hydrated hydrophilic systems.

The lack of the strength gain in the samples that are held in the conditions, where it is impossible to decrease the thickness of the water films (wet), shows the interdependence of the strength and thickness of water films. The drying of the samples, resulting in decreasing the water films thickness, led to an increase of samples strength.

4. Conclusions

1. The LSPh systems of material containing 50 ... 60% of phosphor-gypsum dihydrate, 10% of lime and 40 ... 30% of sandy loam have the best physical-and-mechanical properties and water absorption and softening coefficients.
2. The coefficient of water absorption of the LSPh composite building material increases in proportion to the content of lime and sandy loam. At a constant content of phospho-gypsum, minimal water absorption is at 10% of lime, which corresponds to the 5th, 10th, and 14th compositions.
3. At a constant content of 50%, 60%, 70% of phosphor-gypsum and variable lime and sandy loam, parameters of ultimate compressive strength reach a maximum of 4 ... 5 MPa at 10…20% of lime and 30 ... 40% of sandy loam (hardening in normal-wet conditions).
4. At hardening in normal-wet conditions, the LSPh samples of composite building material reach only 40% of the indexes of the final ultimate compression strength in dry conditions. Therefore, it is advisable, in our opinion, to carry out hardening of such systems in dry conditions.
5. At hardening the LSPh composite building material, the phase of plaster of Paris is transformed into the phase of dihydrate gypsum. When pressing between the planes of portlandite crystals, phosphor-gypsum, quartz, clay, fluorides, phosphates, sulphates, hydro-sulphates there occur the processes of jointing with the appearance of contacts of concretion, penetration, contiguity, with the formation of crystallization structures and van-der-Waals forces of interaction.
6. The distances between some of the crystallization planes reach approximately $1 \cdot 10^{-7}$ m. This well confirms the hypothesis that if the water films thickness on the surface of the hydrated hydrophilic particles is $10^{-7} \ldots 10^{-9}$ m, then, in this case the transition occurs through the threshold from the wedging pressure to overcoming the forces promoting the attraction of the particles to each other and the appearance of the strength properties in these materials.
7. The drying of the obtained materials at temperatures of 60 … 65 °C results in decreasing the thickness of the water films between the particles and contributes to further increase of the strength. The hardening in dry conditions leads to the decrease in the thickness of water films, increase in the number, to the strength of crystallization contacts between the particles of different dispersion (from 50 mcm to nano-sized) and to a significant strength growth of the LSPh composite material being obtained.
8. According to the X-ray-phase analysis, the effect of crystal hydrate growth of new formations was not noticed, therefore, it can be assumed that the strength is created by the presence of water films with nano-sized thickness.
9. The hypothesis that the thickness of the water films influence the formation of nano- and microstructures for quartz surfaces at temperatures of 60 … 65 °C was confirmed and well work in any hydrated hydrophilic systems.
10. The understanding of the influence of the water films thickness on the processes of the structural formation of hydrated hydrophilic systems makes it possible to predict that the various processing methods, leading to decreasing their thickness, will result in increasing the growth of durable and other characteristics of materials obtained by the unroasted technology.

References

[1] Rashad A M 2015 *Journal of cleaner production* **17** pp 717-25
[2] Liu L, Zhang Y and Tan K 2015 *Advances in cement research* **27** pp 567-70
[3] Hua S, Wang K and Yao X 2016 *Construction and building materials* **8** pp 290-99
[4] Yoon S, Mun K and Hyung W 2015 *Journal of asian architecture and building engineering* **9** pp 189-95
[5] Shen Y, Qian J and Huang Y 2015 *Cement & concrete composites* **12** pp 67-75
[6] Shen Y and Qian J 2015 *Advances in cement research* **4** pp 515-25
[7] Bouchhima L, Rouis M J and Choura M 2017 *Revista romana de materiale-romanian journal of materials* **9** pp 106-11
[8] Hua S, Wang K and Yao X 2015 *Cement & concrete composites* **12** pp 299-308

[9] Lyashkevich IM, Raptunovich GS and Polak AF 1985 *Izv. Vuzov. Ser. Str-vo i arkhitektura* **12** pp 60-63
[10] Shmelev G D 1998 PhD Thesis (Voronezh) 256 p
[11] Petropavlovskaya V B, Belov V V and Buryanov A F 2007 *Stroitelnyye materialy* **12** pp 46-47
[12] Potapov Y B, Zolotukhin S N and Semenov V N 2003 *Stroitelnyye materialy* **7** pp 237-39
[13] Kukina O B 2002 PhD Thesis (Voronezh) 186 p
[14] Zolotukhin S N 1990 PhD Thesis (Voronezh) 178 p
[15] Zolotukhin S N, Ibragim F, Savenkova E A, Solovyeva E A, Lobosok AS, Abramenko A A, Drapalyuk A A and Potapov Y B 2016 *Syryevaya smes dlya izgotovleniya stroitelnykh izdeliy po bezobzhigovoy tekhnologii* (Russian Federation Patent na izobreteniye 2584018)
[16] Semenov V N 2002 PhD Thesis (Voronezh) 144 p
[17] Bachauskene MK 1985 PhD Thesis Kaunas 286 p
[18] Stonis SN 1985 *Problemy proizvodstva ekstraktsionnoy fosfornoy kisloty i okhrany prirody* (Moscow: NIUIF) 107 p
[19] Deryagin BV, Churayev NV and Muller VP 1985 *Poverkhnostnyye sily* (M.: Nauka) 398 p
[20] Deryagin BV et al. 1989 *Voda v dispersnykh sistemakh* (Moscow: Khimiya) 288 p